Convergence in quantum transport calculations: Localized atomic orbitals versus nonlocalized basis sets

J. A. Driscoll and K. Varga
Department of Physics and Astronomy, Vanderbilt University, Nashville, Tennessee 37235, USA
(Received 14 December 2009; published 9 March 2010)

The convergence and basis set dependence of quantum transport calculations is studied using localized atomic orbitals and nonlocalized basis sets. The nonequilibrium Green's function formalism and ground-state density-functional theory are used in the calculations. Numerical examples show that the extended nonlocalized basis sets give more accurate results with much lower basis dimension than the atomic orbitals. Examples also show that a low-dimensional atomic orbital basis can also be accurate provided that the self-consistent ground-state potential is accurately calculated.

DOI: 10.1103/PhysRevB.81.115412 PACS number(s): 73.40.−c, 85.65.+h, 72.10.−d, 73.63.−b

I. INTRODUCTION

The convergence of energy and other physical properties in ground-state electronic structure calculations has been intensively studied in the past. Benchmark calculations have been established and state of the art electronic structure calculations are validated against them. Depending on the basis states used in the calculation there are various ways to control the convergence. In plane-wave calculations[1] the convergence of the energy is controlled by the energy cutoff. In real-space grid calculations[2–6] convergence can be reached by increasing the number of grid points. Convergence of calculations using atomic orbitals are checked against the increase in the number of orbitals in the basis.

The convergence of the conductance or the transmission coefficient in quantum transport calculations[7–20] is more complicated. There is no simple minimum principle (such as the minimum of the variational energy in ground-state calculations) that can be used to judge the quality of the calculations. Most quantum transport calculations are based on the nonequilibrium Green's function (NEGF) formalism which, in its most common implementation, uses localized basis sets. The basis set dependence of these calculations is obviously a very important issue. Nevertheless, only a very few calculations have investigated the convergence of the transmission coefficient as a function of the basis size.[21,22] In Ref. 21 Gaussian-based atomic orbitals were used and the convergence with respect to the number of Gaussian orbitals was investigated for a model gold-benzenedithiolate-gold structure. In Ref. 22 several test systems were used and both atomic orbitals (SIESTA)[23] and Wannier function-based basis functions were tested. The slow convergence of the transport properties with localized atomic orbitals is apparent in both calculations. The main reason behind the slow convergence of atomic orbital-based calculations is that it is hard to represent the rapidly oscillating extended current-carrying states with localized orbitals centered on the atoms.

In this work the convergence of transport properties is investigated using different basis sets. Three different basis sets, (1) localized atomic orbitals (AOs), (2) AOs augmented with floating Gaussians, and (3) box basis functions are tested. The first set, the AO basis, is very popular in transport calculations and most transport codes use this representation. These basis functions are centered at atomic positions and give a very good description of the wave function near the atoms (where they are optimized), but the AO representation of the wave function between atoms is less flexible. The advantage of these basis sets is that they are localized and this localization property can be exploited to speed up large scale electronic structure calculations. On the other hand, these basis sets cannot be systematically enlarged in a simple way and the results are subject to basis set errors. To improve the description of the electron scattering wave function in the space between atoms one can augment the atomic orbitals in the interstitial region with suitably chosen basis functions. In this work we add a grid of "floating" Gaussian functions to improve the representation of the wave function between atoms. The third set, the "box basis functions" consists of basis functions that are obtained by diagonalizing the Hamiltonian in an appropriately chosen region (box). Unlike the AOs these basis functions are not tied to atomic positions and are proven to be an efficient representation for electronic structure and transport calculations.[24]

To calculate the transport properties the NEGF formalism is used in the density-functional theory (DFT) framework.[7–19] In the NEGF implementation one has to have basis states that do not connect the left and right leads and it is also advantageous to have basis functions that only connect the nearest periodically repeated layers in the lead. The basis function sets employed in this work satisfy both of these conditions.

The transport calculation has two steps. First the ground-state density and potential are calculated self-consistently and then, using this self-consistent potential, the NEGF formalism is used to calculate the transmission as a function of energy. The accuracy of both of these steps depends on the basis set chosen. The basis set dependence of the ground-state DFT calculation has been extensively researched in the past.[25,26] The main objective of the present work is to investigate the basis set dependence of the second step, the transmission calculation, which consists of the calculation of the Green's function of the system in a suitable basis representation.

The paper is organized as follows. Following the introduction, Sec. II gives a brief presentation of the transport formalism and the definition of the basis states. Numerical

examples are presented in Sec. III and a summary is given in Sec. IV.

II. FORMALISM

In this section we briefly describe the calculation of the transmission coefficients and describe the definition of the basis function sets used in the calculations.

A. Calculation of the Transmission Coefficient

In the NEGF framework the system is divided into left and right leads and a device part as shown in Fig. 1.

The leads consist of periodically repeated layers (boxes). The Hamiltonian is defined as

$$H_{KS} = \frac{-\hbar^2}{2m}\nabla^2 + V_A(\mathbf{r}) + V_H[\rho](\mathbf{r}) + V_{xc}[\rho](\mathbf{r}), \tag{1}$$

where V_A is the Coulomb potential of the atomic nuclei, V_H is the Hartree potential, and V_{xc} is the exchange-correlation potential.

Each region is represented by a set of basis functions Ψ^L, Ψ^C, and Ψ^R. Here the index $X=L,C,R$ refers to the fact that these basis functions are situated in the $X=L,C,R$ (left, center, and right) regions. As has been discussed, only neighboring regions overlap, that is

$$\langle \Psi_i^L | \Psi_j^C \rangle \neq 0 \quad \langle \Psi_i^R | \Psi_j^C \rangle \neq 0, \tag{2}$$

but there is no overlap between the leads' basis functions

$$\langle \Psi_R | \Psi_L \rangle = 0. \tag{3}$$

In this basis representation the Hamiltonian and the overlap matrices of the left-lead—device—right-lead system, under the assumption that there is no interaction between the leads, takes the form

$$H = \begin{pmatrix} H_L & H_{LC} & 0 \\ H_{LC}^\dagger & H_C & H_{RC}^\dagger \\ 0 & H_{RC} & H_R \end{pmatrix} \quad O = \begin{pmatrix} O_L & O_{LC} & 0 \\ O_{LC}^\dagger & O_C & O_{RC}^\dagger \\ 0 & O_{RC} & O_R \end{pmatrix},$$

where $H_L(O_L)$, $H_C(O_C)$, and $H_R(O_R)$ are the Hamiltonian (overlap) matrices of the leads and the device. $H_{LC}(O_{LC})$ and $H_{RC}(O_{RC})$ are the coupling matrices between the central region and the leads defined as

$$H_{ij}^{XY} = \langle \Psi_i^X | H_{KS} | \Psi_j^Y \rangle \quad O_{ij}^{XY} = \langle \Psi_i^X | \Psi_j^Y \rangle. \tag{4}$$

By defining the self energies of the leads $(X=L,R)$ as

$$\Gamma_X(E) = i[\Sigma_X(E) - \Sigma_X^\dagger(E)], \tag{5}$$

where

$$\Sigma_X(E) = (EO_{XC} - H_{XC}) g_X(E) (EO_{XC} - H_{XC}), \tag{6}$$

and where

$$g_X(E) = (EO_X - H_X)^{-1}, \tag{7}$$

is the Green's function of the semi-infinite leads and defining the Green's function of the central region

$$G_C(E) = [EO_C - H_C - \Sigma_L(E) - \Sigma_R(E)]^{-1}, \tag{8}$$

the transmission probability is given by[7]

$$T(E) = Tr[G_C(E)\Gamma_L(E)G_C^\dagger(E)\Gamma_R(E)]. \tag{9}$$

In this equation the transmission coefficient, $T(E)$, is expressed by the Green's functions of the device and the semi-infinite leads. The Green's function of the semi-infinite leads, g_X, is calculated by the decimation[27] technique.

B. Basis Functions

In the following two subsections we briefly introduce the basis functions used in the calculations.

1. Localized orbitals

The atomic orbitals are defined as

$$\phi_{k\alpha}^{AO}(\mathbf{r} - \mathbf{R_k}) = \sum_j c_{pj} \varphi_{lm}^{\nu_j}(\mathbf{r} - \mathbf{R_k}) \tag{10}$$

where $\mathbf{R}_k$ is the position of atom k and α is an index for (p,l,m). Gaussian functions are used in the expansion of the atomic orbitals

$$\varphi_{lm}^{\nu}(\mathbf{r}) = \left(\frac{4\pi 4^l}{(2l+1)!!}\right)^{1/2} (\sqrt{\nu} r)^l \left(\frac{2\nu}{\pi}\right)^{3/4} e^{-\nu r^2} Y_{lm}(\hat{r}).$$

The linear combination coefficients c_{pi} are determined by solving the Kohn-Sham equation for a single atom confined in a sphere of radius R_{cutoff},[28–31] and the AOs vanish beyond that radius. AOs similar to these are very popular in electronic structure and transport calculations. The AO basis depends on the maximum angular momentum l_{max}, the cut-off radius R_{cutoff}, and the maximum number p_{max} of radial parts for each value of the angular momentum l. By increasing l_{max} and p_{max} the accuracy of the calculations improves but the computational time also increases, losing the advantages of the localized basis states. The accuracy of the calculations also depends on the cutoff radius and shape of the AOs. For the light elements used in the present work $R_{cutoff}=5$ Å and $l_{max}=2$ give well-converged results.[25,30]

AOs have proven to be accurate in describing ground-state properties. The AO representation, however, is less flexible for extended continuum wave functions that describe tunneling and current-carrying states. One way to alleviate this is to augment the localized AO with a basis set that flexibly represents the wave functions in the interatomic regions. For this purpose we introduce a grid of Gaussians with $l=0$,

$$\phi_\beta^{grid}(\mathbf{r}) = \varphi_{00}^{\nu}(\mathbf{r} - \mathbf{s_k}), \tag{11}$$

where s_k is a point on a grid where the Gaussian is centered and β is an index for $(\nu,\mathbf{s}_k)$. The grid points $\mathbf{s}_k$ and the Gaussian width parameter ν are selected in such a way that the overlap between neighboring functions is small and there is no linear dependence in the basis. The accuracy of the calculations can be increased by increasing the number of grid points for appropriately chosen ν parameters. Grids of Gaussians are often used as a basis; a recent illustration of

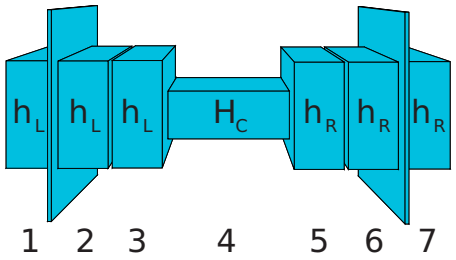

FIG. 1. (Color online) Organization of the system into left/right leads (L/R) and a central device (c). The self-consistent potential is calculated for the central region between the planes. Only a few layers of the leads need to be included to obtain a converged potential for the central region.

the applicability of such functions to represent unbound electrons in nanoelectronics can be found in Ref. 32.

Both of these basis sets are localized in a radius around their centers. In the next subsection we introduce a basis set that is not tied to the atomic positions and is nonzero in a larger spatial region.

2. Box basis functions

In this subsection we define box basis functions as an alternative to the AO representation. These basis functions are defined in each box (see Fig. 1). The jth basis function in the ith box is expanded in terms of a tensorial product of Lagrange basis functions[33] as

$$\phi_j^{box,i}(\mathbf{r}) = \sum_{l=1}^{M_x^i} \sum_{m=1}^{M_y} \sum_{n=1}^{M_z} C_{j,lmn}^i L_l^i(x) L_m(y) L_n(z). \quad (12)$$

In the x direction, the Lagrange functions are defined on grid points $a_i - h < x_k^i < b_i + h$, where a_i is the left and b_i is the right boundary of box i, as

$$L_n^i(x) = \pi_n(x)\sqrt{w(x)} \quad \pi_n(x) = \prod_{\substack{k=1 \\ k\neq n}}^{M_x} \frac{x - x_k^i}{x_n^i - x_k^i}, \quad (13)$$

where $w(x)$ is the weight function and the index i indicates that the Lagrange function is defined in the ith box. The Lagrange functions in neighboring boxes can overlap and the region of overlap is determined by the parameter h. We use the same Lagrange basis $L_m(y)$ and $L_n(z)$ in the y and z directions in each box. By this construction there are $M_i = M_x^i \times M_y \times M_z$ Lagrange basis functions in box i. These functions are used to generate the box basis functions that are used in the transport calculations.

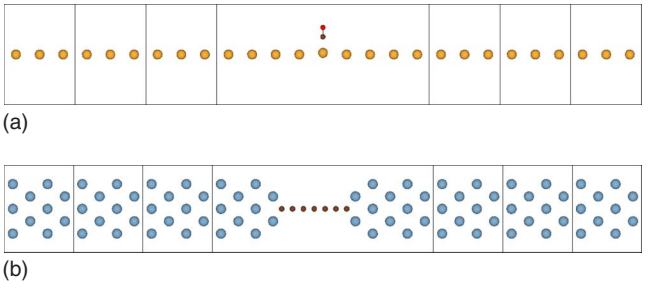

FIG. 2. (Color online) Structure of the (a) Au-CO and (b) Al-C-Al systems. The division into lead and device regions, displayed generally in Fig. 1, is shown.

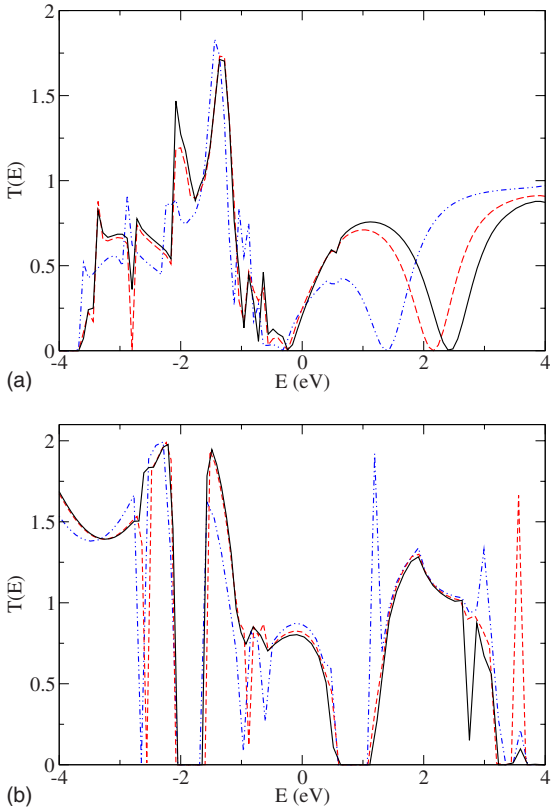

FIG. 3. (Color online) Transmission vs relative energy for the (a) Au-CO and (b) Al-C-Al systems using an atomic orbital basis. In these plots, both the ground state and the conductance calculations were performed on the same AO basis (p_{max}=1 blue dot-dashed line, p_{max}=2 red dashed line, and p_{max}=3 black solid line).

The box basis functions $\phi_j^{box,i}$ are selected by solving the eigenvalue problem

$$H_i C_j^i = E_j C_j^i, \quad (14)$$

where H_i is the matrix of the Hamiltonian H_{KS} in the ith box in the orthogonal Lagrange function representation. After diagonalization this Hamiltonian has M_i eigenstates. By using a cutoff energy E_{cutoff} the lowest n_i eigenstates of this Hamiltonian are used as box basis states in the transport calculations. The convergence properties and accuracy of this approach has been studied in Ref. 24.

III. NUMERICAL RESULTS

Two systems were used to study the convergence of transport calculations. The Au-CO system is a linear chain of Au atoms to which a CO molecule has been adsorbed. This system has been studied in Ref. 22 and we adopted the geometry of the atoms from that source. The other system, Al-C-Al, consists of two bulk Al leads joined by a linear chain of seven carbon atoms (Fig. 2). The Al lattice constant is

TABLE I. Convergence of conductance (in units of G_0). The asterisk appears when the basis size was too large to complete the calculation. N_C and N_L denotes the basis dimension in the central region and in the unit cell of the lead.

		Au-CO			Al-C-Al		
		N_C	N_L	G	N_C	N_L	G
Case I	$p_{max}=1$	99	27	0.244	423	162	0.868
	$p_{max}=2$	198	54	0.248	846	324	0.819
	$p_{max}=3$	297	81	0.208	1269	486	0.788
	$p_{max}=4$	396	108	0.204	1692	648	*
	$p_{max}=5$	495	135	0.212	2115	810	*
Case II	$p_{max}=1$	99	27	0.185	423	162	0.739
	$p_{max}=2$	198	54	0.078	846	324	0.693
	$p_{max}=3$	297	81	0.039	1269	486	0.817
	$p_{max}=4$	396	108	0.017	1692	648	0.874
	$p_{max}=5$	495	135	0.001	2115	810	0.902
Case III	1	50	25	0.001	100	50	0.721
	2	60	30	0.001	120	60	0.755
	3	70	35	0.001	140	70	0.762
	4	80	40	0.001	160	80	0.763
	5	100	50	0.001	180	90	0.763

4.05 Å, the distance of the C atoms from the Al surfaces is 1 Å, and the C-C distance is 1.25 Å

These are relatively simple systems but they allow us to study the convergence properties using large basis sets. The increased computational cost associated with systems that contain more atoms would prevent us from a systematic enlargement of the bases.

In the calculations we first determine the self-consistent potential by diagonalizing the Kohn-Sham Hamiltonian [Eq. (1)] in the region that includes three layers in the left, three layers in the right, and the central region (see Fig. 2) using periodic boundary conditions on the computational cell.

Numerical tests show that adding these three layers is sufficient to obtain the converged self-consistent potential in the middle region containing layers 2–3, the device and layers 5–6 (between the planes in Fig. 2). The self-consistent potential obtained in this way does not change in the middle region if further layers are included in the computational cell. That is, this self-consistent potential is the same as it is in the infinite system containing the semi-infinite leads and the device. Using the self-consistent potential of this middle region one can calculate the matrix elements needed in the transmission calculations using the basis functions defined above.

First we calculated the transmission coefficient using AOs. In these calculations both the self-consistent ground state and the transmission coefficient are calculated using the same AO basis set; that is, the transmission coefficient has a twofold dependence on the basis set.

There are three parameters that influence the convergence behavior: R_{cutoff}, l_{max}, and p_{max}. Out of the three, p_{max}, the number of orbitals per angular momentum, is the most sensible to vary and the easiest to change. We have kept $l_{max}=2$ and $R_{cutoff}=5$ Å as these are typical choices in AO calculations and give good ground-state properties for these systems. Figure 3 shows the transmission as a function of energy (relative to the Fermi energy) for $p_{max}=1,2,3$. Considering the value of the transmission at the Fermi energy, the calculated conductances are shown in Table I (Case I). The transmission curves obtained for different p_{max} values are quite different, and the convergence as a function of the number of basis states is slow, similar to what has been observed in previous calculations.[21,22] For clarity Fig. 3 only shows the results up to $p_{max}=3$, as the transmission for $p_{max}=4$ and $p_{max}=5$ is still changing; that is, convergence has not been reached. Adding more AOs is difficult because the computational time becomes prohibitively large. The slow convergence is especially noticeable in the Au-CO case. The somewhat better convergence in the Al-C-Al case is due to the fact that the d $l=2$ states are included in these calculations. Without the d states, a truncation that is often used in transport calculations, the convergence is much worse. The inclusion of the d states is computationally demanding and by omitting them, the basis dimensions would decrease to less than half of what is shown in Table I. The convergence of the conductances in the table shows a very similar pattern to what has been discussed above concerning the transmission curves.

Next, we will study the effect of varying the basis just in the transmission calculation, and leaving the ground state basis fixed. To this end we calculate the self-consistent potential without employing AOs, instead using the Lagrange function method[33] which provides an accurate self-consistent potential. Any other approach, e.g., plane-wave basis calculations could have been used for this purpose; the main point is that the self-consistent potential has been calculated independently of the basis function sets that are to be tested in the transmission calculations. For all subsequent calcula-

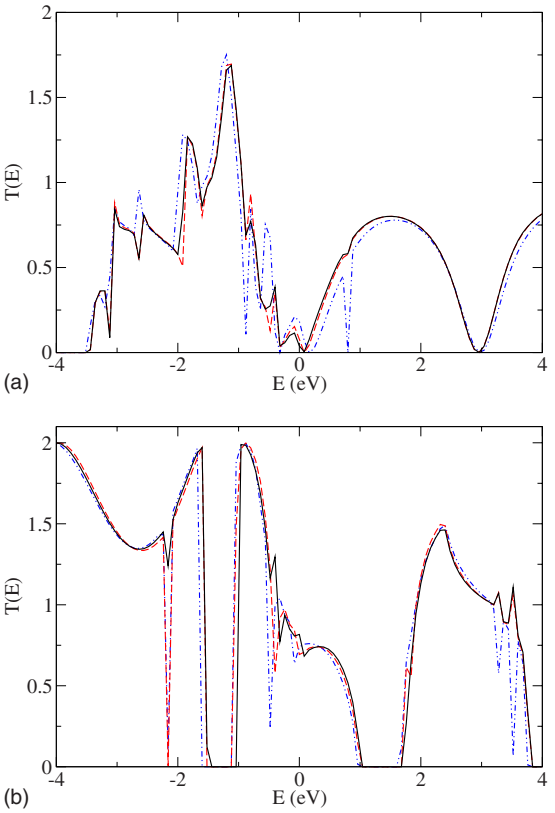

FIG. 4. (Color online) Transmission vs relative energy for the (a) Au-CO and (b) Al-C-Al systems using an atomic orbital basis. In contrast with Fig. 3, here the ground-state potentials for all curves were the same, calculated with a Lagrange basis for high accuracy.

tions, we will fix the ground-state potential to that obtained by the Lagrange function basis. This allows us to see just the influence of varying the AO basis in the transmission calculation.

Figure 4 shows the basis set dependence of the AO-based calculation for the fixed self-consistent potential. Compared to the previous case, the convergence is much faster and a much smaller basis set is sufficient to calculate accurate transport properties. The conductance values in Table I (Case II) nicely converge with the number of basis states. One can notice that the converged values are different from those

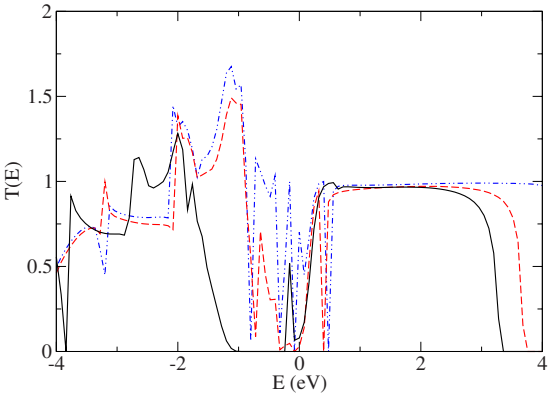

FIG. 5. (Color online) Same as Fig. 4(a), except that the atomic orbital bases used were spatially smaller.

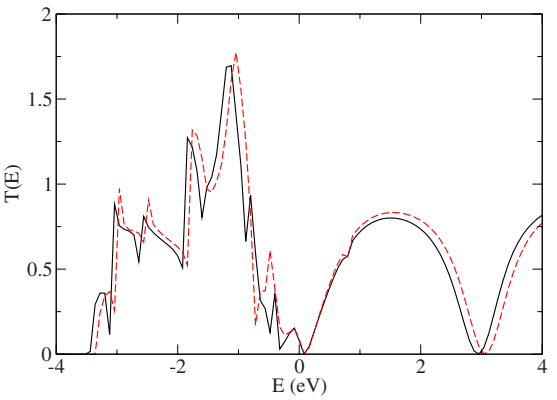

FIG. 6. (Color online) Au-CO transmission calculation with the Gaussian-augmented AO basis. For $p_{max}=2$ the transmission is calculated with (dashed red line) and without (solid black line) the addition of a uniform grid of Gaussian basis functions.

shown in Case I. This shows that a large part of the basis set error in the previous case is due to the basis set dependence of the self-consistent potential. This is mostly due to the difference of the Fermi energies obtained by the Lagrange basis grid and by the AO self-consistent potential calculations. Due to the Fermi energy difference the curves are

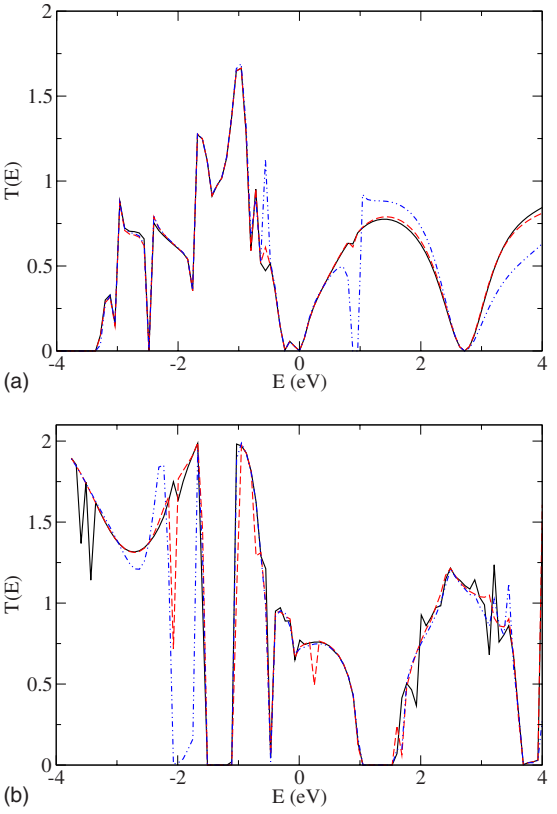

FIG. 7. (Color online) Convergence of the transmission using box basis states for (a) Au-CO and (b) Al-C-Al. The curves correspond to the number of box basis states as defined by sets 1 (blue dot-dashed line), 2 (red dashed line), and 3 (black solid line) in Table I (Case III). The results obtained by using larger basis sets (4 and 5 in Table I) are identical with the black solid line within the resolution of the figure.

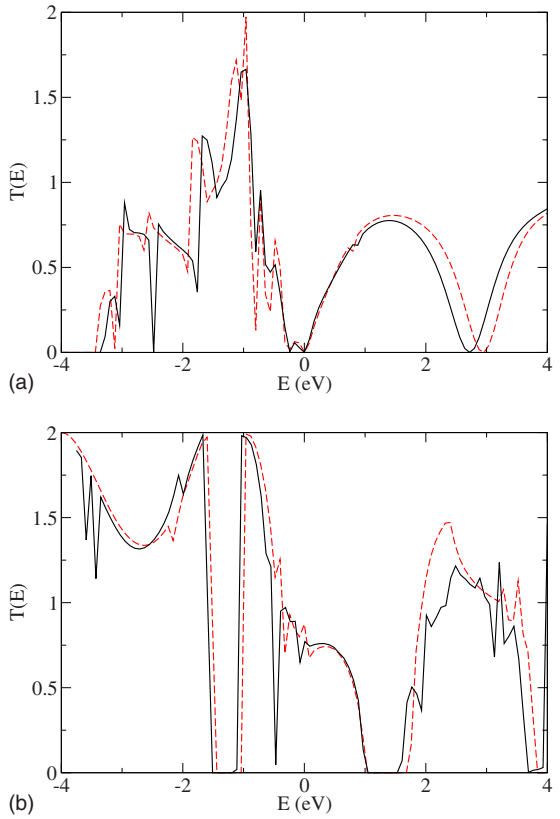

FIG. 8. (Color online) Comparison of the results obtained by the box basis (solid black line) and the AO (dashed red line) for (a) Au-CO and (b) Al-C-Al.

slightly shifted leading to this shift in the conductances. It is interesting to note the strong dependence of the results on R_{cutoff}. Figure 5 shows the same calculation as Fig. 4(a) using AOs with R_{cutoff}=3.5 Å. The smaller radius does not significantly affect the energy of the system, but the calculated transmission has substantially changed, especially in the higher energy region.

We have also investigated the effect of augmenting the AO with floating Gaussian states. The calculations show that these states do not significantly improve the convergence. For example, adding a grid of Gaussians to p_{max}=2 (Fig. 6) does not substantially change the transmission coefficient. Adding a Gaussian grid to AOs which have a smaller cutoff radius changes the results somewhat more (these results are not shown here) but it is found to be hard to optimize their positions and widths. Moreover, although adding floating Gaussians have somewhat changed the transmission coefficients, no clear convergence pattern could be found.

Next we show our results using the box basis states. The convergence of the transmission is shown in Fig. 7 and the conductances can be seen in Table I (Case III). The most important result of this case is that the transmission converges rapidly and systematically as a function of the number of basis states. One can also note that the number of basis states needed for convergence is much less than in the AO calculations. The converged box basis calculation is compared to the best AO results in Fig. 8. The agreement is good; for a better agreement probably more AOs should be included, which as we have already emphasized, is computationally unfeasible.

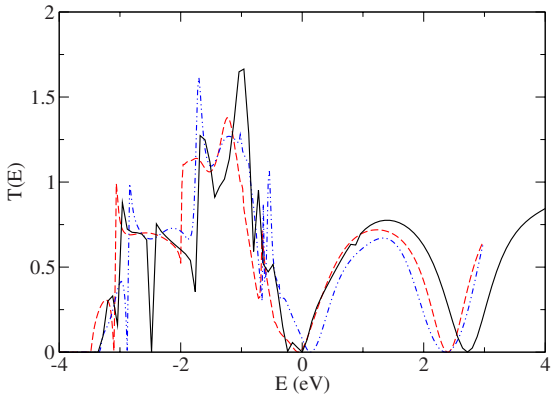

FIG. 9. (Color online) Comparison of the box basis calculation (solid black line) to benchmark results. The blue dot-dashed line is the Wannier, the red dashed line is the AO calculation of Ref. 22.

Finally, we compare our results to the benchmark calculation published in Ref. 22. In the benchmark paper the transmission functions are calculated using two different density functional theory methods, an ultrasoft pseudopotential plane-wave code in combination with maximally localized Wannier functions and the norm-conserving pseudopotential code SIESTA which applies an atomic orbital basis set. Figure 9 compares the results of the benchmark calculation to our box basis results. The agreement is very good.

IV. CONCLUSIONS AND SUMMARY

The development of efficient quantum transport calculations[7–20] is an area of very active research. These calculations have yet to reach the accuracy and efficacy of ground state DFT calculations. Using the combination of the nonequilibrium Green's function formalism and ground-state density-functional theory we have studied the convergence and basis set dependence of quantum transport calculations.

Atomic orbitals are widely used in NEGF implementations, but the convergence of transport properties with respect to the number of basis states is slow. Examples in this paper show that this is partly due to the basis set dependence of the self-consistent potential. In other words, if the self-consistent potential is accurately calculated then much fewer AOs are needed in the calculation of the transport properties. The calculation of the transport coefficient is a time consuming part of the transport calculations because it involves many inversions of large matrices and this has to be repeated for many energy values.

The box basis orbitals lead to much faster convergence on a much smaller basis than the AOs. The typical number of basis states per electron orbital is about 2–3. This significantly reduces the computational cost. Another useful property of the box basis is that by increasing the number of basis states the Hilbert space is enlarged and the transport coefficients systematically converge. In the case of AOs the transport coefficients always change and due to computational limitations the same level of accuracy cannot be reached.

The accuracy of box basis states is due to the facts that (1) they are spatially extended and can represent scattering states efficiently and (2) the box basis states are optimized for the converged self-consistent potential.

The present calculations are restricted to zero bias voltage. The study of transport calculations in nonequilibrium conditions is more challenging and left for future work.

ACKNOWLEDGMENTS

This work is supported by NSF grants No. ECCS0925422 and No. CMMI0927345.

[1] M. C. Payne, M. P. Teter, D. C. Allan, T. A. Arias, and J. D. Joannopoulos, Rev. Mod. Phys. **64**, 1045 (1992).
[2] T. Hoshi, M. Arai, and T. Fujiwara, Phys. Rev. B **52**, R5459 (1995).
[3] E. L. Briggs, D. J. Sullivan, and J. Bernholc, Phys. Rev. B **54**, 14362 (1996).
[4] T. L. Beck, Rev. Mod. Phys. **72**, 1041 (2000).
[5] M. Heiskanen, T. Torsti, M. J. Puska, and R. M. Nieminen, Phys. Rev. B **63**, 245106 (2001).
[6] J. R. Chelikowsky, N. Troullier, K. Wu, and Y. Saad, Phys. Rev. B **50**, 11355 (1994).
[7] S. Datta, *Electronic Transport in Mesoscopic Systems* (Cambridge University Press, New York, 1997).
[8] S. V. Faleev, F. Léonard, D. A. Stewart, and M. van Schilfgaarde, Phys. Rev. B **71**, 195422 (2005).
[9] J. J. Palacios, A. J. Pérez-Jiménez, E. Louis, E. SanFabián, and J. A. Vergés, Phys. Rev. Lett. **90**, 106801 (2003).
[10] K. Stokbro, J. Taylor, M. Brandbyge, J. L. Mozos, and P. Ordejón, Comput. Mater. Sci. **27**, 151 (2003).
[11] E. G. Emberly and G. Kirczenow, Phys. Rev. B **64**, 235412 (2001).
[12] J. Taylor, H. Guo, and J. Wang, Phys. Rev. B **63**, 245407 (2001).
[13] M. B. Nardelli, J.-L. Fattebert, and J. Bernholc, Phys. Rev. B **64**, 245423 (2001).
[14] Y. Xue, S. Datta, and M. A. Ratner, J. Chem. Phys. **115**, 4292 (2001).
[15] K. Thygesen and K. Jacobsen, Chem. Phys. **319**, 111 (2005).
[16] S.-H. Ke, H. U. Baranger, and W. Yang, Phys. Rev. B **70**, 085410 (2004).
[17] P. Derosa and J. Seminario, J. Phys. Chem. B **105**, 471 (2001).
[18] X. Zhang, L. Fonseca, and A. A. Demkov, Phys. Status Solidi B **233**, 70 (2002).
[19] S. Sanvito, C. J. Lambert, J. H. Jefferson, and A. M. Bratkovsky, Phys. Rev. B **59**, 11936 (1999).
[20] A. Garcia-Lekue and L. Wang, Comput. Mater. Sci. **45**, 1016 (2009).
[21] C. W. Bauschlicher, Jr., J. W. Lawson, A. Ricca, Y. Xue, and M. A. Ratner, Chem. Phys. Lett. **388**, 427 (2004).
[22] M. Strange, I. S. Kristensen, K. S. Thygesen, and K. W. Jacobsen, J. Chem. Phys. **128**, 114714 (2008).
[23] P. Ordejón, E. Artacho, and J. M. Soler, Phys. Rev. B **53**, R10441 (1996).
[24] K. Varga, Phys. Rev. B **81**, 045109 (2010).
[25] M. Gusso, J. Chem. Phys. **128**, 044102 (2008).
[26] J. S. Nelson, E. B. Stechel, A. F. Wright, S. J. Plimpton, P. A. Schultz, and M. P. Sears, Phys. Rev. B **52**, 9354 (1995).
[27] M. P. L. Sancho, J. M. L. Sancho, and J. Rubio, J. Phys. F: Met. Phys. **15**, 851 (1985).
[28] T. Ozaki and H. Kino, Phys. Rev. B **69**, 195113 (2004).
[29] J. Junquera, O. Paz, D. Sánchez-Portal, and E. Artacho, Phys. Rev. B **64**, 235111 (2001).
[30] V. Blum, R. Gehrke, F. Hanke, P. Havu, V. Havu, X. Ren, K. Reuter, and M. Scheffler, Comput. Phys. Commun. **180**, 2175 (2009).
[31] O. F. Sankey and D. J. Niklewski, Phys. Rev. B **40**, 3979 (1989).
[32] D. Soriano, D. Jacob, and J. J. Palacios, J. Chem. Phys. **128**, 074108 (2008).
[33] K. Varga, Z. Zhang, and S. T. Pantelides, Phys. Rev. Lett. **93**, 176403 (2004).